JACS Au
AN OPEN ACCESS JOURNAL OF THE AMERICAN CHEMICAL SOCIETY

pubs.acs.org/jacsau
Article

Catalytic Hydrodeoxygenation of Mixed Plastic Wastes into Sustainable Naphthenes

Jieyi Liu,‖ Nan Wang,‖ Sibao Liu,* and Guozhu Liu*

Cite This: JACS Au 2024, 4, 4361−4373
Read Online
ACCESS | Metrics & More | Article Recommendations | Supporting Information

ABSTRACT: The chemical upcycling of plastic wastes by converting them into valuable fuels and chemicals represents a sustainable approach as opposed to landfilling and incineration. However, it encounters challenges in dealing with mixed plastic wastes due to their complex composition and sorting/cleaning costs. Here, we present a one-pot hydrodeoxygenation (HDO) method for converting mixed plastic wastes containing poly(ethylene terephthalate) (PET), polycarbonate (PC), and poly(phenylene oxide) (PPO) into sustainable naphthenes under mild reaction conditions. To facilitate this process, we developed a cost-effective, contaminant-tolerant, and reusable Ni/HZSM-5 bifunctional catalyst through an ethylene glycol-assisted impregnation method. The metallic Ni site plays a pivotal role in catalyzing C−O and C−C cleavages as well as hydrogenation reactions, while the acidic site of HZSM-5 facilitates dehydration and isomerization reactions. The collaboration between metal and acid dual sites on Ni/HZSM-5 enabled efficient HDO of a wide range of substrates, including bottles, textile fibers, pellets, sheets, CDs/DVDs, and plastics without cleaning or pigments removal and even their various mixtures, into naphthenes with a high yield up to 99% at 250 °C and 4 MPa H_2 within 4−6 h. Furthermore, the metal-acid balance of the Ni/HZSM-5 catalyst is crucial for determining both HDO activity and product distribution. This proposed one-pot HDO process utilizing earth-abundant metal catalysts provides a promising avenue toward practical valorization of mixed plastic wastes.

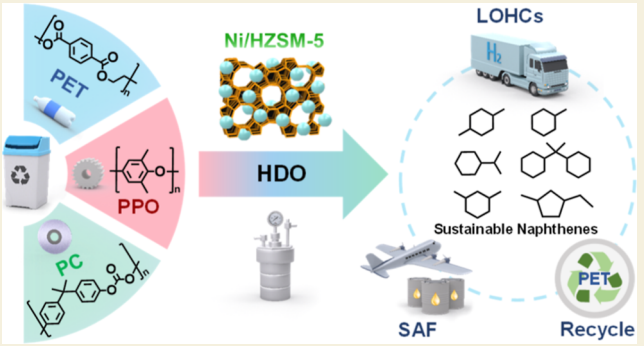

KEYWORDS: *plastic wastes, hydrodeoxygenation, naphthene, Ni, ZSM-5*

INTRODUCTION

The global annual production of plastics has now exceeded 400 million tons, and this quantity is projected to experience a substantial increase over the forthcoming decades, ultimately reaching 1231 million tons by 2060.[1] During production and usage, a significant amount of plastic waste is generated and accumulated. Among various commodity plastics, oxygen-containing aromatic polymers, such as polyethylene terephthalate (PET), polycarbonate (PC), and polyphenyl ether (PPO), constitute more than 10% of the total postconsumer plastic waste.[1,2] Unfortunately, the majority of plastic waste is directly disposed in landfills or incinerated, resulting in severe environmental pollution and loss of carbon resources.[2−5] Recycling these plastic wastes presents a promising approach to address both concerns; however, less than 10% have been recycled thus far.[6−8] Physical recycling currently represents the predominant method, which necessitates sorting and cleaning steps for obtaining pure polymers but often leads to performance degradation in most plastics.[7,9,10] On the other hand, chemical recycling/upcycling offers a more promising solution for efficiently utilizing plastic waste as valuable carbon resources by converting them into valuable fuels and chemicals.[11−17] At present, the common chemical recycling method for converting oxygen-containing aromatic plastic wastes involves monomer production through different chemistries, including hydrolysis, alcoholysis, glycolysis, and amination.[18] Nevertheless, these processes encounter numerous challenges, such as the need for abundant solvents, difficult recovery of homogeneous acid−base catalysts, and purification difficulties in obtaining high-quality monomers.[19,20] Therefore, innovative chemical strategies for the production of valuable new products are the key to enrich the utilization of these plastic wastes.

Recently, various strategies have been developed for the upcycling individual oxygen-containing aromatic plastic wastes (PET, PC, and PPO), including hydrogenolysis,[19−22] hydrodeoxygenation (HDO),[23−28] and CO_2-assisted depolymerization.[29,30] Among these transformation methods, HDO shows great potential in selectively producing high-value naphthenes

Received: August 4, 2024
Revised: October 5, 2024
Accepted: October 7, 2024
Published: October 11, 2024

https://doi.org/10.1021/jacsau.4c00701
JACS Au 2024, 4, 4361−4373

by saturating benzene rings and breaking C−O bonds (Figure 1). Specifically, HDO of PET yields targeted 1,4-dimethylcyclohexane; HDO of PC produces propane-2,2-diyldicyclohexane; and HDO of PPO results in 1,3-dimethylcyclohexane. These naphthenes are important chemical products with potential applications as sustainable aviation fuels (SAF)[31,32] and liquid organic hydrogen carriers (LOHCs).[24,33] Moreover, 1,4-dimethylcycloalkane can serve as a promising reagent for terephthalic acid production through dehydrogenation and oxidation processes. This reagent can subsequently be used for PET reproduction to achieve closed-loop PET recycling. The easy separation of cycloalkanes effectively addresses purification issues during monomer production from PET plastic waste. Consequently, the production of naphthenes via HDO from plastic waste offers a new pathway for SAF synthesis, sustainable LOHCs production, and closed-loop PET recycling (Figure 1).

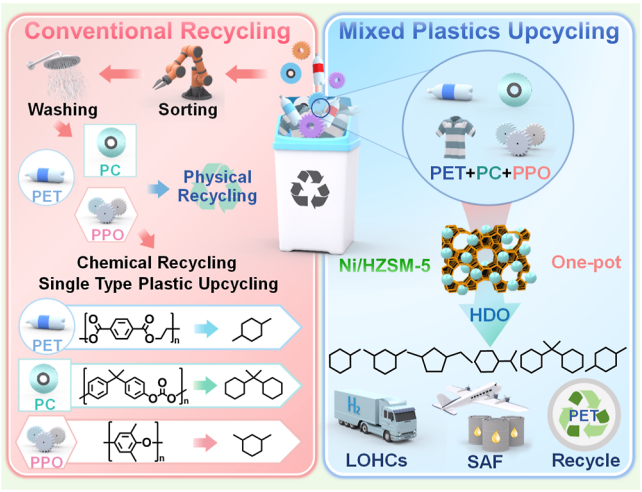

Figure 1. Schematic illustration of plastic wastes recycling/upcycling: conventional plastic wastes recycling vs mixed plastic upcycling by the one-pot HDO process.

The oxygen-containing aromatic plastic wastes are formed by connecting aromatic monomers through different types of C−O bonds, such as PET and PC, which are connected by ester C−O bonds, while PPO is connected by ether C−O bonds. Therefore, the challenge in the HDO of these plastic wastes to produce naphthenes lies in how to construct an efficient HDO catalytic system that can achieve precise activation and cleavage of C−O bonds while preserving the C−C bond. Currently reported processes for producing cyclic alkanes from HDO, include multistep methods[34−36] and one-pot methods.[24,37−40] Compared to the multistep method, the one-pot method is simpler and more efficient. The reported catalytic systems are mainly noble metal-based catalytic systems, including Rh/C + USY,[37,41] Ru/TiO_2,[27,38] Ru−Ni/Hβ,[40] Pd/C + La(Otf)$_3$,[39] and Ru−ReO_x/SiO_2 + HZSM-5.[24] Despite the advancements, several challenges remain to be addressed in catalytic processes for plastic waste conversion. First, while most current methods focus on transforming single-component plastic wastes, the treatment of real-world mixed plastic wastes remains challenging due to their complex composition and diverse C−O bonds.[24,42,43] However, the conversion of individual plastic wastes could require costly sorting and separation steps. Only one study has reported that the Ru−ReO_x/SiO_2 + HZSM-5 catalytic system can convert mixed oxygen-containing plastic wastes into cycloalkanes;[24] however, it only achieves a yield of approximately 70% for naphthenes after a reaction time as long as 30 h. Moreover, the use of noble metals can significantly limit practical applications due to their expense. To date, there is no non-noble metal catalyst that can convert multiple types of individual and mixed plastics into naphthenes with high yields in a short time. Second, real-world plastic wastes often contain contaminants and additives, such as food residue and pigments. These impurities can poison catalysts and lead to deactivation, which makes upcycling real-world plastic wastes more challenging.[44] Additional purification steps are required in most reported catalytic systems, which could increase costs. However, there is no study that can enable the HDO of real-world mixed plastic wastes with contaminants to yield naphthenes in high yields. Third, there is currently no effective catalytic system available for HDO of PPO linked with inert etheric C−O bonds into naphthenes.[24] Furthermore, global textile waste recycling rates are less than 0.5%, and the main component of these textiles is PET.[45,46] HDO of postconsumer textile fibers into naphthenes could provide a new route for upcycling textile wastes. However, it remains an area that has received limited attention. Lastly, the detailed reaction pathway for HDO of plastic waste into cycloalkanes, particularly regarding PET conversion, is still insufficiently understood. To address the above issues, it is imperative to develop robust noble-metal-free catalysts that can be compatible with a wide variety of substrates, particularly mixed plastic wastes, while being tolerant toward various impurities.

In this study, we have developed a highly efficient Ni/HZSM-5 bifunctional catalyst for one-pot HDO of PET, PC, and PPO and their mixtures into sustainable naphthenes under mild reaction conditions (Figure 1). This catalyst demonstrated an exceptional ability in converting a wide range of plastic substrates, including bottles, textile fibers, pellets, sheets, CDs/DVDs, plastics with colorants, and plastics without prior cleaning. Remarkably, it also exhibited superior performance in complete HDO of various mixed plastic wastes containing food residues and pigments to produce high yield of naphthenes up to 99% at 250 °C and 4 MPa H_2 within a short reaction time of 4−6 h. Moreover, this catalyst showed excellent stability, as it can be reused at least 6 times without any loss in activity. Mechanistically, the detailed reaction pathway for the HDO of PET and PPO into naphthenes has been elucidated. The synergy between metal and acid sites on Ni/HZSM-5 is crucial in achieving high HDO activity, while the balance between metal and acid sites can be tuned for tailoring product distribution. This innovative approach provides a promising solution for effectively upcycling mixed plastic wastes toward practical implementation.

RESULTS AND DISCUSSION

Catalyst Screening for the HDO of PET

PET was initially selected as the substrate for catalyst screening in the HDO reaction, which was carried out at a temperature of 240 °C and a H_2 pressure of 4 MPa H_2 for 6 h using cyclopentane as the solvent. Initially, different Ni/zeolite catalysts, including Ni/HZSM-5(25), Ni/HY(25), and Ni/Hβ(25) with the same SiO_2/Al_2O_3 ratio, were screened (Figure S1). All of the catalysts were active for the HDO of PET into naphthenes, resulting in the production of various cycloalkanes, including 1,4-dimethylcyclohexnae (DMCH),

https://doi.org/10.1021/jacsau.4c00701
JACS Au 2024, 4, 4361−4373

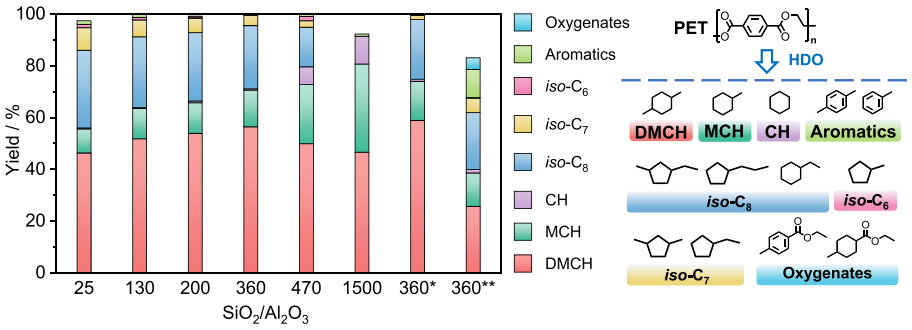

Figure 2. HDO of PET over Ni/HZSM-5 catalysts with different SiO_2/Al_2O_3 ratios. Reaction condition: catalyst: 0.3 g, PET: 0.3 g, cyclopentane: 15 mL, T: 240 °C, 6 h, 500 rpm, initial H_2: 4 MPa. *4 h. **catalyst: Ni/HZSM-5(360)-NE catalyst prepared without the addition of EG, 4 h.

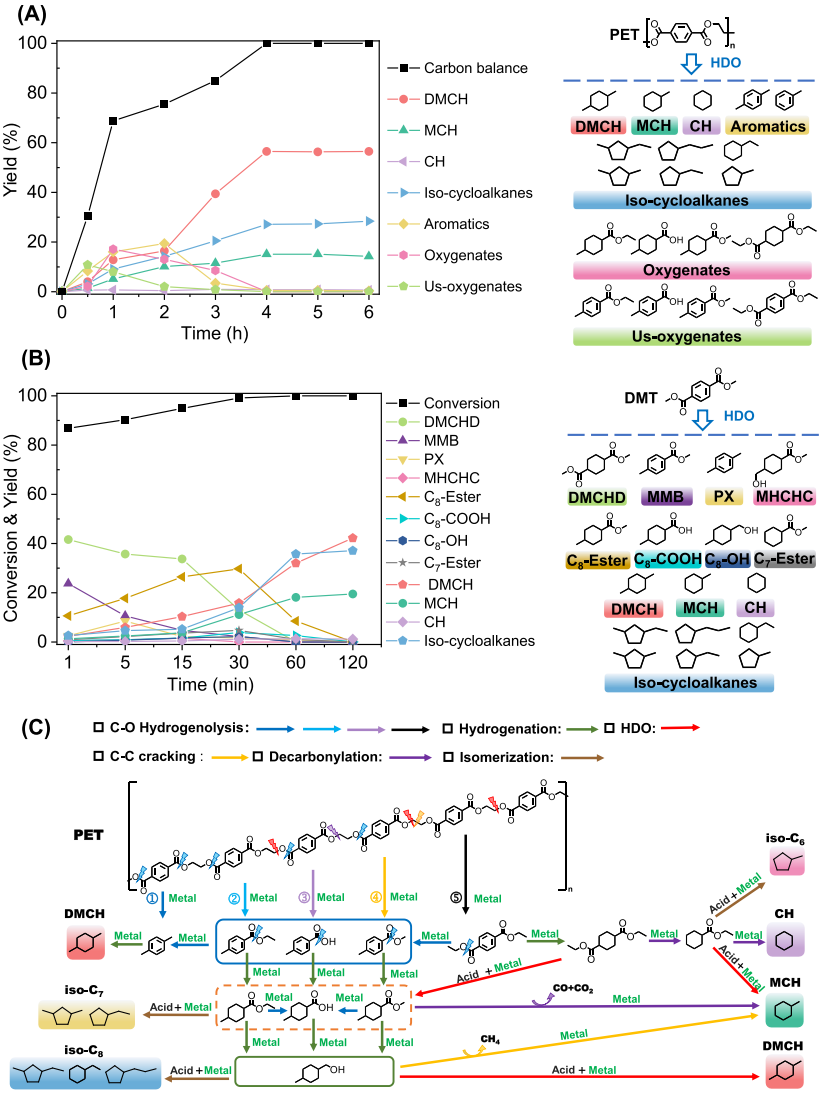

Figure 3. (A) Reaction profile of PET over the Ni/HZSM-5(360) catalyst. (B) Reaction profile of dimethyl terephthalate (DMT) over the Ni/HZSM-5(360) catalyst. (C) Reaction pathway for HDO of PET over the Ni/HZSM-5(360) catalyst. Reaction condition: catalyst: 0.3 g, reactant: 0.3 g, cyclopentane: 15 mL, T: 240 °C, 6 h, 500 rpm, initial H_2: 4 MPa and (B) initial N_2: 0.5 MPa, H_2: 4 MPa.

methylcyclohexane (MCH), cyclohexane (CH), isomeric cycloalkanes (iso-C_8, iso-C_7, and iso-C_6), and aromatics. 1,4-Dimethylcycloalkane (DMCH) is the target product from HDO of PET without carbon loss. Isomeric cycloalkanes refer to structurally distinct products compared to DMCH, MCH, and CH, primarily composed of five-membered rings. The yield of naphthenes followed the order of Ni/HZSM-5(25) > Ni/Hβ(25) > Ni/HY(25). This indicated that the HZSM-5 zeolite as the support showed superior HDO activity. Therefore, it was selected as the support for further investigations. Next, the performances of the Ni/HZSM-5 catalysts with different SiO_2/Al_2O_3 ratios were studied. As depicted in Figure 2, increasing the SiO_2/Al_2O_3 ratio from 25 to 360 in Ni/HZSM-5 catalysts resulted in a total yield

https://doi.org/10.1021/jacsau.4c00701
JACS Au 2024, 4, 4361−4373

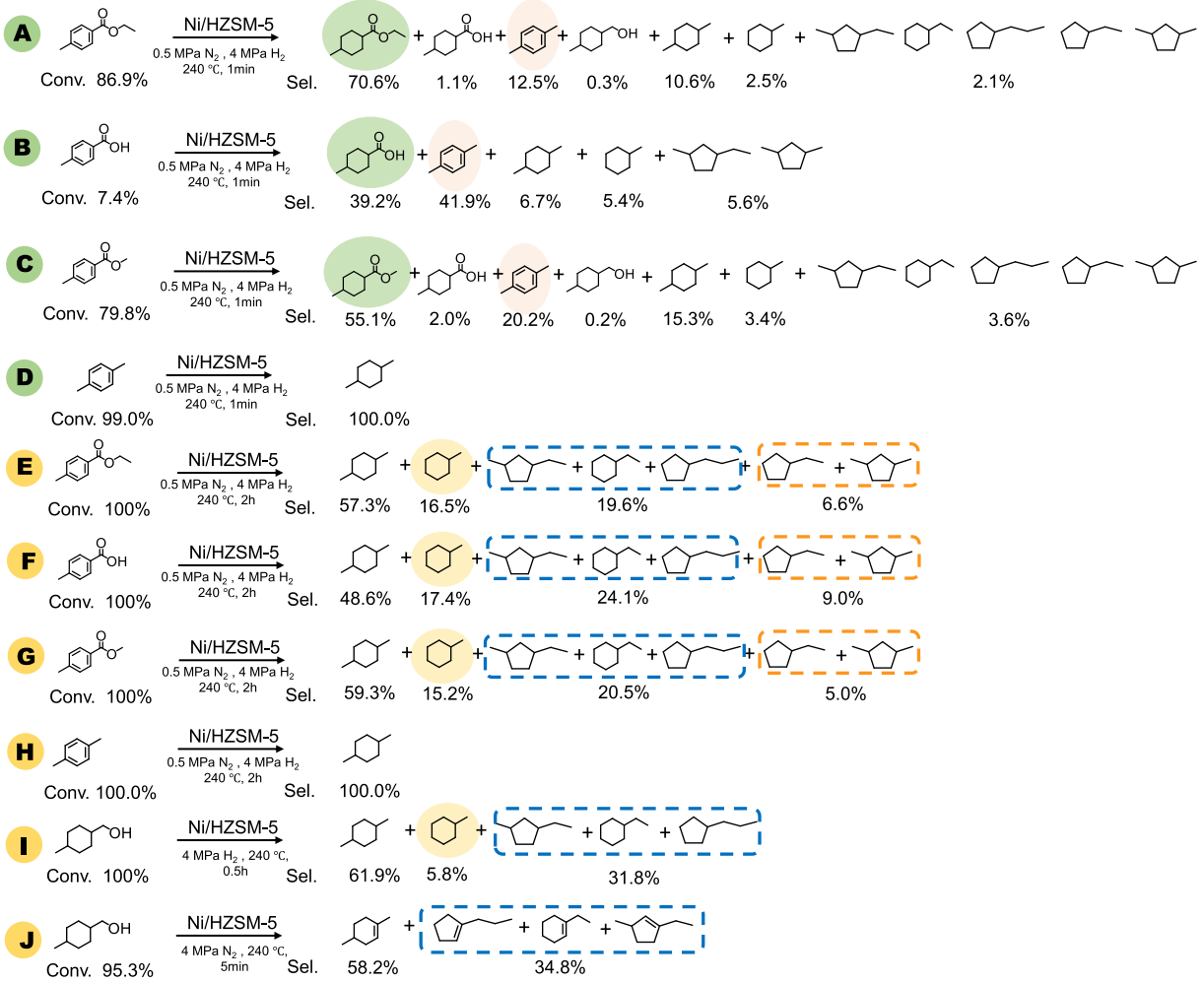

Figure 4. HDO of various model compounds over the Ni/HZSM-5(360) catalyst. Reaction condition: catalyst: 0.3 g, reactant: 0.3 g and cyclopentane: 15 mL, T: 240 °C, 500 rpm.

increase of cycloalkanes up to 99.6%, accompanied by a significant rise in the yield of target DMCH while it reduced that of isomeric cycloalkanes. However, further increasing SiO_2/Al_2O_3 to 1500 led to a decrease in a DMCH yield along with a substantial increase in MCH and CH yields. Additionally, there was a significant reduction in the isomeric cycloalkane yield due to insufficient acidic sites on the zeolite with high SiO_2/Al_2O_3 ratios. Among all tested catalysts, Ni/HZSM-5(360) with a SiO_2/Al_2O_3 ratio of 360 achieved the highest yield for both total cycloalkanes (99.6%) and DMCH (56.4%), which was chosen for further research. The conversion of PET with HZSM-5 alone showed that PET almost cannot be converted, and a very trace amount of the products was detected (Figure S1), indicating that the addition of HZSM-5 does not play a role in the depolymerization of PET. This suggested the crucial role of Ni metal in the HDO reaction.

Compared to the Ni/HZSM-5(360)-NE catalyst prepared without the addition of EG, Ni/HZSM-5(360) showed higher HDO activity (Figure 2). After a reaction time of 4 h, the total yield of naphthenes was only 67.7%, which is much lower than that (99.9%) over Ni-HZSM-5(360). In addition, there was still a certain amount of oxygenates (4.5%) were not converted. X-ray diffraction (XRD), transmission electron microscopy (TEM), and CO-chemisorption analysis revealed that the Ni/HZSM-5(360) catalyst displayed smaller-sized Ni particles with improved dispersion (Figure S2). These findings suggested that the addition of EG during the catalyst preparation promoted the dispersion of Ni particles, thereby enhancing the HDO activity of Ni/HZSM-5. It has been reported that EG can act as a surfactant, facilitating improved wetting of the support and ensuring uniform distribution of the Ni precursor on a HZSM-5 support during the impregnation step.[47] Additionally, owing to its higher viscosity and boiling point in comparison to water, EG and Ni precursors can form a gel-like phase during the drying step, thereby preventing redistribution.[47−49] Moreover, the protective effect of EG could inhibit further growth during the calcination step so that small particles are obtained.[49,50]

Reaction Pathway for the HDO of PET to Naphthenes

In order to elucidate the detailed reaction pathway for the HDO of PET to cycloalkanes, the changes in product distribution with reaction time during HDO of PET over the Ni/HZSM-5(360) catalyst were investigated (Figure 3A). At the very beginning of the reaction, the detected intermediates mainly consisted of unsaturated oxygenates (us-oxygenates), saturated oxygenates (oxygenates), and aromatics (aromatics). Unsaturated oxygenates included ethyl 4-methylbenzoate, 4-methylbenzoic acid, methyl 4-methylbenzoate, and diethyl terephthalate, with ethyl 4-methylbenzoate being the predom-

https://doi.org/10.1021/jacsau.4c00701
JACS Au 2024, 4, 4361−4373

inant product. Saturated oxygenated compounds comprised ethyl 4-methylcyclohexane-1-carboxylate, 4-methylcyclohexanecarboxylic acid, methyl 4-methylcyclohexane-1-carboxylate, and diethyl 1,4-cyclohexanedicarboxylate, with ethyl 4-methylcyclohexane-1-carboxylate being the major product. It is noteworthy that most of the oxygenated products were mono-esters and mono-acids, while trace amounts of diesters, such as diethyl terephthalate and diethyl 1,4-cyclohexanedicarboxylate, were observed at the reaction time of 30 min with yields of 0.7% and 0.3%, respectively. The aromatics were mainly *p*-xylene accompanied by a very small amount of toluene. These intermediates were mainly generated by depolymerization through random C−O and C−C bond cleavages in PET, specifically dominated by C−O bond cleavage. The yields of these intermediates exhibited an initial increase, followed by a decrease over time. In contrast, the yield of the target DMCH showed a linear increase with reaction time, which was accompanied by an increase in the yield of MCH and isomeric cycloalkanes and a very small amount (0.8%) of CH. As shown in Figure S3, the presence of CO_2 and CO was detected in the gaseous product, indicating that decarboxylation and decarbonylation reactions occurred during the conversion of PET to naphthenes, resulting in the loss of C atoms. It is evident that the oxygenated compounds and aromatics that appeared at the early stage were important intermediates for the formation of cycloalkanes. These intermediates were subsequently transformed into DMCH through HDO and hydrogenation reactions, respectively, accompanied by decarboxylation, decarbonylation, and isomerization reactions, thus generating MCH and CH cycloalkanes as well as isomerized cycloalkane products. At a reaction time of 4 h, complete conversion of PET into naphthenes was achieved with an overall yield of 99.9%, including 58.9% of the target product DMCH; 15.9% of MCH and CH as C−C cleavage products; and 25.1% of isomerized cycloalkanes.

To clarify the reaction process for the conversion of these intermediates to cycloalkanes, we performed HDO reactions using some key intermediates (Figure 4). At the initial stage of the HDO reactions, converting unsaturated oxygenated compounds (ethyl 4-methylbenzoate, 4-methylbenzoic acid, and methyl 4-methylbenzoate) over the Ni/HZSM-5(360) catalyst resulted in significant formation of saturated oxygenated compounds along with partial production of *p*-xylene (Figure 4A−C). Additionally, an important intermediate in the HDO reaction, namely, 4-methyl-1-cyclohexanemethanol (C_8−OH) was also detected. Upon complete conversion of these unsaturated oxygenated compounds, DMCH, MCH, and isomeric cycloalkane products were obtained with similar product distributions (Figure 4E−G). The products from HDO of C_8−OH were predominantly DMCH with a certain amount of MCH and isomeric C_8 cycloalkane products (Figure 4I). In contrast, hydrogenation products from *p*-xylene exclusively yielded DMCH without any detectable presence of other byproducts, such as DMCH or isomeric alkanes even at longer reaction time (Figure 4D,H). This indicated that the formation of MCH involved decarboxylation and decarbonylation reactions of carboxylic acid and ester oxygenated intermediates, as well as hydrocracking via C−C cleavage of C_8−OH. In order to understand the production pathway of the isomeric cycloalkanes, we carried out the conversion of C_8−OH using a Ni/HZSM-5(360) catalyst under the N_2 atmosphere and found that the dehydration process occurred (Figure 4J). In addition to the target C_8 cyclo-olefin products, C_8 isomeric cyclo-olefins were also observed (Figure 4J). Therefore, we proposed that the production of these isomeric C_8 cycloalkane products is mainly generated by dehydration-isomerization-hydrogenation of intermediate alcohols. However, the isomerized C_7 cycloalkanes were not detected during the HDO of C_8−OH, confirming that the isomeric C_7 cycloalkane products are produced along with the decarboxylation/carbonylation reactions of oxygenated compounds. In summary, the conversion of aromatic esters and acids to cycloalkanes primarily involves two reaction pathways: (1) hydrogenation saturation of aromatic ester and acid, followed by the HDO of saturated oxygen-containing intermediates to form DMCH. This pathway is accompanied by decarboxylation/carbonylation reactions, C−C bond hydrocracking reactions, and isomerization reactions, resulting in the formation of MCH and isomerization cycloalkanes; (2) C−O hydrogenolysis of aromatic esters to *p*-xylene and subsequent hydrogenation to DMCH. It should be noted that the yield of saturated oxygenated products surpasses that of *p*-xylene significantly (Figure 4A−C), thereby establishing pathway (1) as the predominant route.

To further validate the reaction pathway for HDO of PET, ethyl 4-methylbenzoate (EMB) and DMT were employed as model compounds for conducting time-dependent experiments (Figures 3B and S4). Figure 3B shows the product distribution from HDO of DMT over time. Initially, both benzene ring saturation product [dimethyl 1,4-cyclohexanedicarboxylate-(DMCHD)] and the C−O hydrogenolysis products (methyl 4-methylbenzoate (MMB) and *p*-xylene (PX)) were generated, indicating both benzene ring hydrogenation and C−O hydrogenolysis are the primary routes for initial depolymerization of PET during HDO. The yield of products from benzene ring saturation was significantly higher than that from C−O hydrogenolysis, suggesting the predominance of benzene ring hydrogenation. These observations were further supported by time-dependent experiments using ethyl 4-methylbenzoate (EMB) as a model compound (Figure S4). Additionally, a small amount of methyl 4-hydroxymethylcyclohexane-1-carboxylate (MHCHC) was detected within 1−15 min, which could originate from acyl C−O bond hydrogenolysis in dimethyl 1,4-cyclohexanedicarboxylate (DMCHD). As the reaction progressed, this compound underwent dehydration and subsequent hydrogenation to form methyl 4-methylcyclohexanecarboxylate (C_8−ester). The yield of C_8−ester gradually increased and reached a maximum value of 29.7% at 30 min; meanwhile, a small amount of 4-methylcyclohexanecarboxylic acid (C_8−COOH) was also formed through C−C bond cracking in methyl C_8−ester because no acid product was observed when conducting hydrolysis over Ni/HZSM-5(360). Furthermore, a trace amount of C_8−OH was detected, which can be formed through the hydrogenolysis of the acyl C−O bond in C_8−ester. Additionally, a minor quantity of methyl cyclohexanecarboxylate (C_7−ester), resulting from decarboxylation of DMCHD and cleavage of the C−C bond in MHCHC, was observed during the reaction process. After a reaction time of 120 min, complete conversion of DMT to naphthenes occurred. The yield for the desired product DMCH reached 42.2%, while the yields for MCH and CH were found to be 19.5% and 1.2%, respectively. The yield for isomeric cycloalkanes was determined to be 37.1%. The yield of naphthenes from HDO of DMT could reach 96%, with 57.3% yield of DMCH, 16.5% yield of MCH, and 22.2% yield of isomerized cycloalkanes. It is noted that the product

https://doi.org/10.1021/jacsau.4c00701
JACS Au 2024, 4, 4361−4373

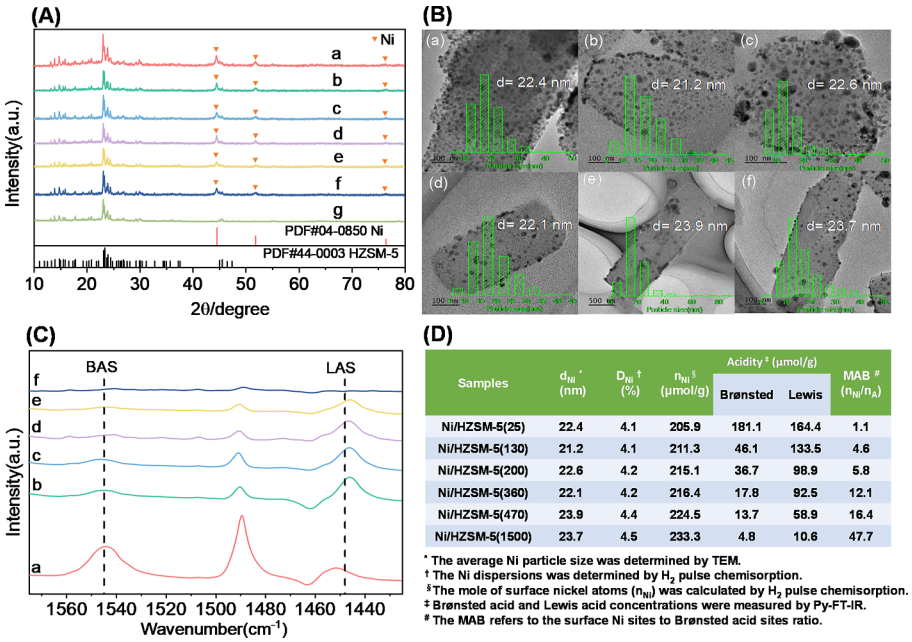

(D)

Samples	d_{Ni} * (nm)	D_{Ni} † (%)	n_{Ni} § (μmol/g)	Acidity ‡ (μmol/g)		MAB # (n_{Ni}/n_A)
				Brønsted	Lewis	
Ni/HZSM-5(25)	22.4	4.1	205.9	181.1	164.4	1.1
Ni/HZSM-5(130)	21.2	4.1	211.3	46.1	133.5	4.6
Ni/HZSM-5(200)	22.6	4.2	215.1	36.7	98.9	5.8
Ni/HZSM-5(360)	22.1	4.2	216.4	17.8	92.5	12.1
Ni/HZSM-5(470)	23.9	4.4	224.5	13.7	58.9	16.4
Ni/HZSM-5(1500)	23.7	4.5	233.3	4.8	10.6	47.7

* The average Ni particle size was determined by TEM.
† The Ni dispersions was determined by H_2 pulse chemisorption.
§ The mole of surface nickel atoms (n_{Ni}) was calculated by H_2 pulse chemisorption.
‡ Brønsted acid and Lewis acid concentrations were measured by Py-FT-IR.
# The MAB refers to the surface Ni sites to Brønsted acid sites ratio.

Figure 5. Characterizations of Ni/HZSM-5 catalysts. (A) XRD patterns and (B) TEM images of reduced (a) Ni/HZSM-5(25), (b) Ni/HZSM-5(130), (c) Ni/HZSM-5(200), (d) Ni/HZSM-5(360), (e) Ni/HZSM-5(470), and (f) Ni/HZSM-5(1500). (C) Py-FT-IR spectra of reduced (a) Ni/HZSM-5(25), (b) Ni/HZSM-5(130), (c) Ni/HZSM-5(200), (d) Ni/HZSM-5(360), (e) Ni/HZSM-5(470), and (f) Ni/HZSM-5(1500). (D) Characterization data of the catalysts.

distribution from HDO of EMB is more close to that from HDO of PET (Figure S4), suggesting that the initial depolymerization of PET to monoester and acid is the dominant route. The reaction routes for the HDO of DMT and EMB were depicted (Figures S4B and S5).

Based on the time-dependent experimental results with PET and model molecules, the reaction pathway for HDO of PET to naphthenes can be inferred (Figure 3C). The conversion of PET into naphthenic hydrocarbons using a Ni/HZSM-5 bifunctional catalyst involves two primary stages: (1) depolymerization of PET macromolecules leading to the formation of various intermediates, including methyl aromatic esters and acids, *p*-xylene, and trace amounts of diethyl terephthalate and (2) subsequent conversion of these intermediate products through HDO and hydrogenation reactions into cycloalkanes. The overall reaction pathway for converting PET into naphthenes encompasses multiple reactions, such as C−O hydrogenolysis, HDO, hydrogenation, decarboxylation/carbonylation, C−C cleavage, and isomerization. First, the depolymerization of PET macromolecules is achieved through C−O hydrogenolysis and C−C bond cleavage at various positions within the PET molecular chain. With catalysis on metal Ni sites, simultaneous random C−O bond hydrogenolysis reactions occur at multiple positions along the macromolecular chain. Depending on the types of C−O bond hydrogenolysis, different aromatic monoesters and mono-acid intermediates can be formed. The acyl C−O (indicated by blue arrow) is more susceptible to undergo hydrogenolysis, resulting in predominantly aromatic monoesters as well as *p*-xylene formation. A trace amount of ethyl terephthalate is also formed due to concurrent hydrogenolysis of the alkyl C−O bond (indicated by red arrow). Additionally, a small number of C−C bond cleavage reactions (indicated by a yellow arrow) occur during PET depolymerization, leading to methyl 4-methylbenzoate formation. The metallic Ni sites in the Ni/HZSM-5 catalyst play a crucial role in initial PET depolymerization through C−O hydrogenolysis and C−C cracking. Enhancing Ni dispersion significantly promotes the depolymerization of PET into small-molecular oxygenated intermediates, as evidenced by higher yields of oxygenated intermediates over Ni/HZSM-5(360) prepared using the EG-assisted impregnation method compared to that over Ni/HZSM-5(360)-NE prepared without EG (Figure S6). The intermediate products from the first stage can be classified into two categories: unsaturated oxygenates (aromatic esters and acids) and *p*-xylene. Based on experimental results with model compounds, some unsaturated oxygenates can also undergo acyl C−O hydrogenolysis to yield *p*-xylene, which was subsequently hydrogenated to form DMCH at metal Ni sites. The majority of unsaturated oxygenated compounds were transformed into cycloalkanes through HDO reactions at metal-acid dual sites. The unsaturated oxygenates were cascade converted to an important intermediate, C_8−OH at metal Ni sites through cascade hydrogenation of the benzene ring and hydrogenolysis of acyl C−O bonds. Subsequently, dehydration occurs on acidic sites leading to the formation of dimethyl cyclohexene, followed by hydrogenation at metal Ni sites resulting in DMCH formation. During the conversion of saturated oxygenates, decarboxylation/carbonyl reactions occurred leading to MCH formation. Furthermore, the C−C bond cleavage reaction of intermediate C_8−OH also took place on metal Ni sites, contributing to MCH formation. According to the reaction pathway for HDO of DMT, the low yield of CH may originate from decarboxylation/decarbonylation reactions of 1,4-cyclohexanedimethanol diethyl ester. Due to the presence of acid sites, saturated oxygen-containing compounds can undergo isomerization reactions during decarboxylation/carbonyl processes and dehydration, resulting in the formation of isomeric cycloalkanes.

https://doi.org/10.1021/jacsau.4c00701
JACS Au 2024, 4, 4361−4373

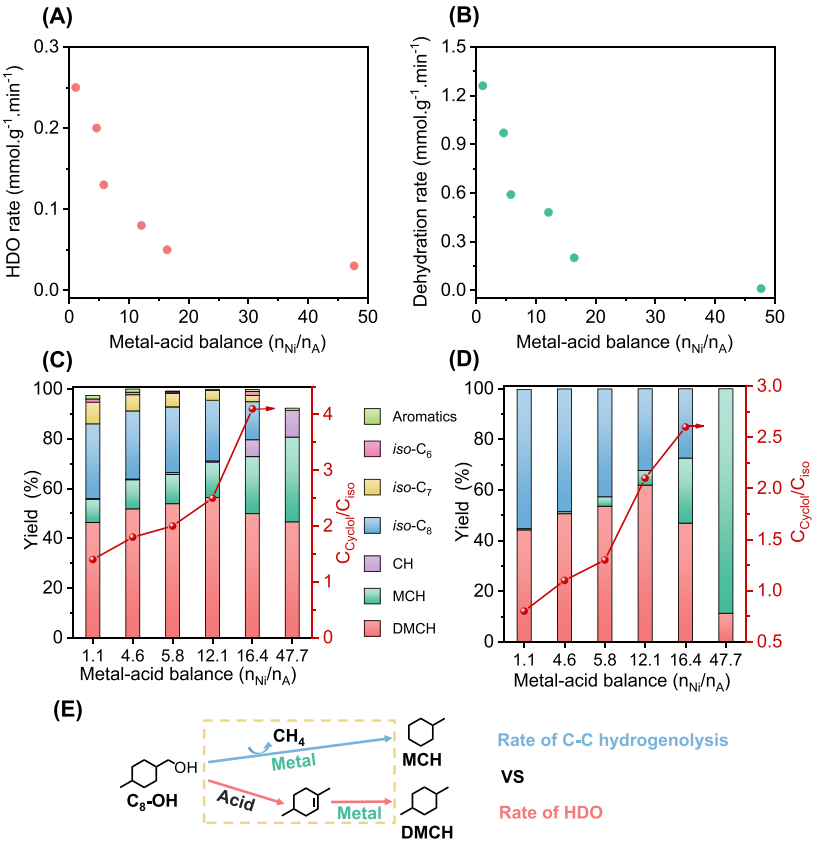

Figure 6. (A) HDO activity of PET as a function of MAB. (B) Dehydration activity of C_8−OH as a function of MAB; HDO product distribution of PET (C) and C_8−OH (D) as a function of the MAB. (E) Reaction pathway for conversion of C_8−OH. (A,C) Reaction condition: catalyst: 0.3 g, PET: 0.3 g and cyclopentane: 15 mL, T: 240 °C, 1 h, 500 rpm, initial H_2: 4 MPa. (B,D) Reaction condition: catalyst: 0.3 g, C_8−OH: 0.3 g and cyclopentane: 15 mL, T: 190 °C, 5 min, 500 rpm, initial N_2: 4 MPa.

Correlation between Metal-Acid Balance (MAB) and Catalytic Performance

XRD analysis revealed that all Ni/HZSM-5 catalysts exhibited characteristic peaks corresponding to MFI-type zeolite zeolites, indicating that the introduction of metallic Ni did not alter the zeolite structure. Diffraction peaks were observed at 2θ = 44.5, 51.8, and 76.4°, which can be attributed to the crystal planes of Ni(111), Ni(200), and Ni(220) respectively, confirming the reduction of Ni to its metallic state (Figure 5A). According to the Scherrer equation, the average particle sizes of Ni of Ni/HZSM-5 with different Si/Al ratios were determined to be follows: 22.4 21.2, 22.6, 22.1, 23.9, and 23.7 nm, respectively, suggesting that all Ni/HZSM-5 catalysts possessed comparable average particle sizes of Ni (Figure 5D). Scanning electron microscopy (SEM) images revealed that the introduction of Ni onto the HZSM-5 catalysts resulted in a roughened surface of the zeolite, indicating successful deposition of Ni particles on the zeolite support (Figure S7). TEM analysis demonstrated that the HZSM-5 zeolite surface was surrounded by Ni particles, suggesting the predominant localization of nickel on the zeolite surface (Figure 5B). Statistical analysis (>300 Ni particles) showed that Ni/HZSM-5 catalysts with identical loadings exhibited similar average particle sizes for nickel (21.2−23.9 nm), consistent with XRD findings. H_2 chemisorption further proved that Ni/HZSM-5 possessed similar metal dispersion (4.1−4.5%). Figure 5C presents Py-FT-IR results for the HZSM-5 zeolites. It is evident that an increase in the SiO_2/Al_2O_3 ratio leads to a gradual reduction in the quantity of Brønsted acid present within the HZSM-5 zeolite. Upon quantitative calculations, it was observed that as the SiO_2/Al_2O_3 ratio increased from 25 to 1500, there was a decrease in Brønsted acid content from 181.8 to 4.8 μmol/g (Figure 5D). The MAB of Ni/HZSM-5 bifunctional catalysts, which refer to the surface metal sites to Brønsted acid site ratio, can be determined based on the results obtained from H_2-chemisorption and Py-FT-IR analyses. With an increase in the SiO_2/Al_2O_3 ratio from 25 to 1500, the MAB of Ni/HZSM-5 catalysts exhibited a significant enhancement from 1.1 to 47.7 (Figure 5D).

As discussed in the reaction pathway for HDO of PET section, the synergistic effect between metal and acid in bifunctional Ni/HZSM-5 catalysts plays a pivotal role in the HDO of PET. The metallic Ni site is responsible for catalyzing C−O and C−C cleavages as well as hydrogenation, while the acidic sites of HZSM-5 facilitate dehydration and isomerization reactions. Consequently, MAB is crucial for determining both the HDO activity and product distribution during PET conversion. Given that all Ni/HZSM-5 catalysts exhibited similar average nickel particle sizes, it becomes possible to decouple the influence of metal properties on the HDO of PET. First, we investigated the MAB effect on HDO activity. We define the formation rate of cycloalkanes as the HDO rate for the catalyst. Interestingly, we observed a decrease in the HDO rate with an increase in MAB (Figure 6A), which aligns with variations observed in C_8−OH dehydration rates (Figure 6B). This observation suggested that acid sites play a critical role in enhancing HDO activity by primarily influencing the dehydration step. Next, the effect of MAB on product

https://doi.org/10.1021/jacsau.4c00701
JACS Au 2024, 4, 4361−4373

distribution was clarified. The products obtained from HDO of PET included the desired product DMCH, as well as byproducts such as MCH and CH, and isomeric cycloalkanes. As shown in Figure 6C, increasing the MAB from 1.1 to 47.7 resulted in an increase in the yield of DMCH from 46.3% to 56.4%, while the yield of MCH increased from 9.3% to 14.2%, and the yield of isomeric cycloalkanes decreased from 38.7% to 28.1%. Further increasing MAB led to a decrease in both the yields of DMCH and isomeric cycloalkanes, but a significant increase in the yield of MCH was observed instead. This trend of changes aligns with what was observed for the products resulting from the HDO of 4-methyl-1-cyclohexanol (Figure 6D). According to the reaction pathways for HDO of PET, two possible routes exist for the conversion of C_8−OH into cycloalkanes (Figure 6E): (1) dehydration to form 1,4-dimethylcyclohexene and subsequently hydrogenation to form DMCH; (2) hydrogenolysis via C−C bond cleavage connected to the hydroxyl group to produce MCH. The C−C hydrogenolysis route aligns with previous literature reports.[27] The aforementioned two routes were in a competition manner. To compare the rates between these two routes, a Ni/Silicalite-1 catalyst without Brønsted acid sites was employed for determining the C−C bond cleavage rate in converting C_8−OH into MCH. It was found that the C−C bond cleavage rate was 0.30 mmol·g^{-1}·min^{-1}, which was significantly lower than the dehydration rate of 1.46 mmol·g^{-1}·min^{-1} (Table S1, entries 7−8). Consequently, the main product from C_8−OH over Ni/HZSM-5 catalysts was DMCH. When the MAB increased to 12.1, there was a gradual decrease in the number of Brønsted acid sites. The dehydration rate of C_8−OH also gradually slowed down, while C−C bond cleavage became more pronounced, resulting in a slight increase in the yield of MCH. However, when the MAB further increased, the dehydration rate significantly decreased and the C−C cracking rate became more evident, leading to a significant decrease in the DMCH yield. At this point, without Brønsted acid sites present, C−C bond hydrogenolysis on metallic Ni sites became dominant, and most of the C_8−OH underwent C−C cracking. This resulted in an increase in the MCH yield up to 88.7%. It is worth noting that as MAB increased, the number of Brønsted acid sites gradually decreased. As a result, the isomerization reactions were slowed down, leading to a gradual decrease in the yield of isomeric alkane products. When MAB reached 47.7, there were no isomeric cycloalkanes present in the products. The trend observed in the yield of isomeric cycloalkanes as a function of MAB corresponded with that in the yield of isomeric C_8 cyclo-olefins from the dehydration of C_8−OH (Figure 6C,D and Table S1). These findings indicate that MAB influences the relative rates of different reaction pathways, thereby altering product distributions.

Catalyst Stability

The stability of catalysts is crucial for their practical application. Initially, the catalyst stability was investigated by utilizing the spent Ni/HZSM-5(360) catalyst after the washing and drying steps (Figure 7). Regrettably, the yield of naphthenes decreased to 89.7% accompanied by a minor presence (3.9%) of oxygenates, indicating catalyst deactivation. TG analysis revealed coke formation on the catalyst surface (Figure S8A), which might account for its deactivation. Consequently, a calcination-reduction method was adopted for regenerating the Ni/HZSM-5(360) catalyst for HDO of PET. The regenerated Ni/HZSM-5(360) catalyst maintained

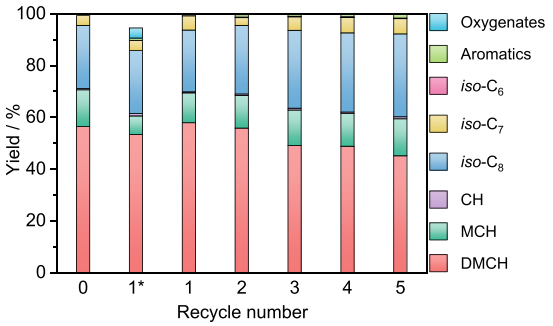

Figure 7. Recyclability of the Ni/HZSM-5(360) catalyst. Reaction condition: catalyst: 0.3 g, PET: 0.3 g, cyclopentane: 15 mL, T: 240 °C, 4 h, 500 rpm, initial H_2: 4 MPa. 1* the spent catalyst without regeneration.

high catalytic activity and exhibited excellent stability. Even after 6 cycles of use, the total yield of cycloalkanes remained above 98%. However, the yield of the target DMCH decreased to 45.1%, while the yield of isomeric cycloalkanes increased by 9.8%. XRD and TEM characterizations were performed on the spent catalyst (Figure S7). In XRD analysis (Figure S8B), sharper diffraction peaks corresponding to metallic nickel in the Ni/HZSM-5(360) catalyst were observed after 6 cycles compared to the freshly reduced catalyst, indicating that sintering of metal particles had occurred. TEM images also showed an increase in particle sizes from 22.1 to 35.8 nm for nickel particles (Figure S8C). These results suggested that after multiple cycles of HDO reactions and regeneration treatments, sintering and agglomeration took place for metallic nickel, resulting in a decrease in MAB, which accelerated isomerization rates and led to an increase in yield of isomeric cycloalkanes.

HDO of Various Real-World Plastic Wastes

The catalytic performance of the Ni/HZSM-5(360) catalyst for processing real-world waste plastics was evaluated. First, we selected commonly encountered PET waste plastics as reaction substrates for HDO experiments (Figure 8A). The reaction substrates included a Coca-Cola bottle, Sprite bottle, and textile fibers. After conducting the reaction at 240 °C and 4 MPa H_2 for 6 h, complete transformation of the cleaned PET bottle was achieved. The total yield of cycloalkanes reached 99.5%, with a specific yield of DMCH at 54.8%. However, practical application costs can be increased by pretreatment steps, such as cleaning; therefore, it is more meaningful to directly treat stained waste plastics without additional cleaning steps. When using a Coca-Cola bottle containing coke stains (PET bottle-dirty) as the reaction substrate under identical reaction conditions, the yield of cycloalkanes could reach up to 98.8%, while maintaining a DMCH yield of 57.8%. Furthermore, the catalyst demonstrated effective conversion capability toward green-pigmented PET Sprite bottle with a cycloalkane yield reaching 99.4%, including a DMCH yield at 52.6%. This suggests that the Ni/HZSM-5 catalyst was tolerant with the colorant in the plastics. Regarding the conversion of textile fibers, this catalyst can effectively transform white fiber into cycloalkanes with an impressive total yield of 99.5% and a DMCH yield of 50.4% at 240 °C, 4 MPa H_2, and 6 h. However, under the same reaction conditions, only a total yield of cycloalkane amounting to 40.0% was observed for HDO of red fiber, with less than 7% yield of DMCH. A significant portion (24.8%) of oxygenates and aromatics

https://doi.org/10.1021/jacsau.4c00701
JACS Au 2024, 4, 4361−4373

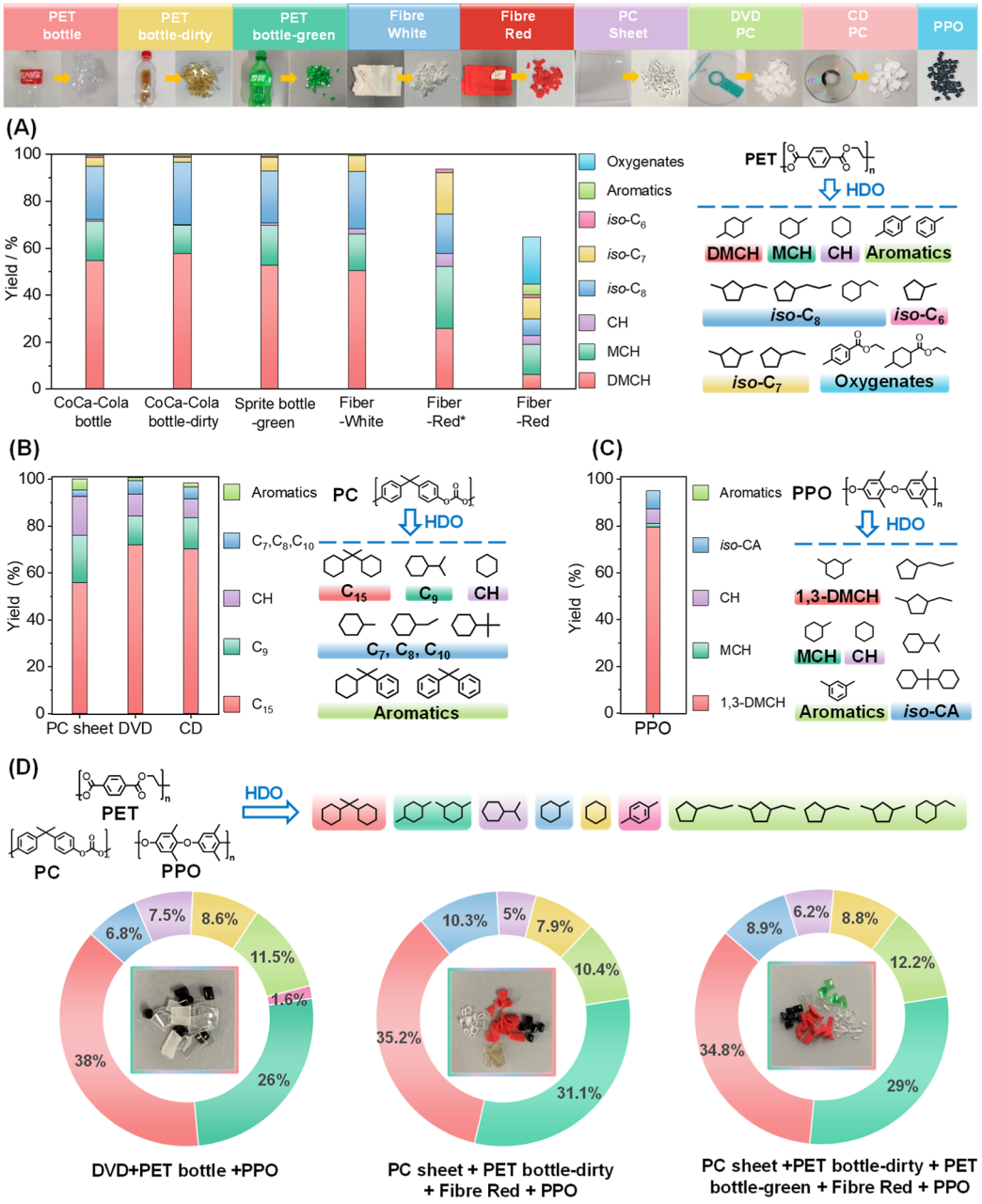

Figure 8. HDO of various real-world PET plastic wastes (A), PC plastic wastes (B), PPO plastic wastes (C), and mixed plastic wastes (D) over the Ni/HZSM-5(360) catalyst. (A,B) Reaction condition: catalyst: 0.3 g, reactant: 0.3 g, cyclopentane: 15 mL, T: 240 °C, 6 h, 500 rpm, initial H_2: 4 MPa. Fiber red*: 12 h. (C,D) Reaction condition: catalyst: 0.3 g, reactant: 0.3 g, cyclopentane: 15 mL, T: 250 °C, 4 h, 500 rpm, initial H_2: 4 MPa. For the mixed plastic wastes, Reactant: 0.1 g PC + 0.1 g PET + 0.1 g PPO. Reaction time for HDO of mixed plastic wastes (PC sheet + PET bottle-dirty + fiber red + PPO) and HDO of mixed plastic wastes (PC sheet + PET bottle-dirty + PET bottle-green + fiber red + PPO): 6 h.

remained unconverted. This discrepancy may be attributed to the inhibitory effect exerted by the red pigment in the red fiber on the catalyst's activity. To address this issue, we extended the reaction time to 12 h and achieved complete conversion of red fiber with an increased total yield of cycloalkanes reaching up to 95.3%, accompanied by a high DMCH yield of 25.8%. The product distribution differed from other PET plastics possibly due to the poisoning effects caused by the basic nitrogen-containing red pigment on acidic sites of HZSM-5 (Figure S9).[45] These results demonstrated that the Ni/HZSM-5(360) catalyst exhibited superior processing capabilities for various types of real-world PET plastic wastes and displayed tolerance toward food stains and pigments.

Subsequently, we investigated the utilization of the Ni/HZSM-5(360) catalyst for HDO of other types of oxygenated aromatic plastic wastes, encompassing poly(bisphenol A carbonate) (PC) and poly(phenylene oxide) (PPO) (Figure 8B,C). The real-world PC plastic waste samples comprising CD, DVD, and a transparent PC sheet were chosen (Figure 8B). Remarkably, all types of PC plastic wastes exhibited complete conversion over the Ni/HZSM-5(360) catalyst with a remarkable yield exceeding 95% in cycloalkanes at 240 °C and 4 MPa H_2 for 6 h. Notably, when CD and DVD were employed as substrates, C_{15} bicycloalkane yields reached approximately 70%. Moreover, isomerized cycloalkanes featuring five-membered rings were not detected during the HDO of

https://doi.org/10.1021/jacsau.4c00701
JACS Au 2024, 4, 4361−4373

PC. The reaction pathway for the conversion of PC into cycloalkanes has been elucidated in our previous work,[51] wherein the depolymerization of PC predominantly occurred through hydrogenolysis of C−O bonds adjacent to benzene rings. The recycling of PPO plastic waste, one of the top five engineering plastics, also was investigated (Figures 8C and S10). Unlike PET and PC, PPO has a structure linked with ether bonds instead of ester groups. Initially, the reaction conditions for PET HDO were adopted (240 °C, 4 MPa H_2, 6 h reaction time) (Figure S10). The overall yield of cycloalkanes observed after HDO of PPO was only 59.7% with a specific yield of the desired 1,3-DMCH at 43.7%. Extending the reaction time to 12 h enhanced the total cycloalkanes yield to 68.5%, with an improved 1,3-DMCH yield of 52.2% (Figure S10). To achieve higher yields, the reaction temperature was further elevated to 250 °C and, upon a reaction time of 4 h, complete conversion of PPO into cycloalkanes was achieved with a remarkable total yield reaching up to 95%, including an impressive 1,3-DMCH yield of 79.4% (Figure 8C). Consequently, by appropriately elevating the reaction temperature, the Ni/HZSM-5(360) catalyst effectively facilitated the transformation of PPO into valuable cycloalkanes. The reaction pathway for HDO of PPO was also evaluated through time-dependent experiments (Figure S11A). During the PPO depolymerization process, simultaneous hydrogenolysis of both C(m)−O and C(o)−O bonds occurs (Figure S11B). However, due to steric hindrance effects, the hydrogenolysis of the C(m)−O bond predominates over that of the C(o)−O bond as the dissociation energy of the latter is higher than that of the former. Subsequently, 2,6-dimethylcyclohexanol and 3,5-dimethylcyclohexanol undergo hydrodeoxygenation reactions to yield 2,6-DMCH.

In practical applications, the efficient treatment of mixed plastic wastes can save costs caused by sorting and washing. To explore the potential application of Ni/HZSM-5(360) catalyst in HDO of mixed plastic wastes, different combinations of real-world PET, PC, and PPO plastic wastes were used as substrates (Figure 8D). Under the conditions of 250 °C and 4 MPa H_2 for 4−6 h, different combinations of mixed plastic wastes can be completely converted. When the reaction substrates were a clean PET bottle, PC (DVD), and PPO, the total yield of cycloalkanes reached 98.4%, with the yield of C_{15} bicyclic alkane at 26.0%, C_8 cycloalkanes at 38.0%, C_6, C_7, and C_9 cycloalkanes at 23.6%, and isomeric cycloalkanes at 11.5%. When the reaction substrates included the PC sheet, dirty PET bottle, red fiber cloth, and PPO, the total yield of cycloalkanes reached 100%, with a yield of C_{15} bicyclic alkane at 31.1%, C_8 alkanes at 35.2%, C_6, C_7, and C_9 cycloalkane at 23.2%, and isomeric cycloalkanes at 10.4%. When the reaction substrates were further adjusted to the combination of PC sheet, green PET bottle, dirty PET bottle, red fiber cloth, and PPO, the total yield of cycloalkanes reached 100.0%, with a yield of C_{15} bicyclic alkane at 29.0%, C_8 cycloalkanes at 34.8%, C_6, C_7, and C_9 cycloalkanes at 23.9%, and isomeric cycloalkanes at 12.2%. The above results demonstrate that the Ni/HZSM-5(360) catalyst is a promising non-noble metal, impurity-tolerant HDO catalyst for efficient HDO of various real-world mixed waste plastics into cycloalkanes in high yields.

CONCLUSIONS

We have successfully demonstrated a noble-metal-free, contaminant-tolerant, and reusable Ni/HZSM-5 catalyst for the one-pot HDO of oxygen-containing aromatic plastic wastes, such as PET, PC, and PPO, as well as their various mixed plastic wastes into sustainable naphthenes under mild reaction conditions. The synergistic effect between the metal sites and acid sites on Ni/HZSM-5 plays a critical role in achieving highly efficient HDO of ester C−O bonds and ether C−O bonds present in various polymers. The metallic Ni site plays a pivotal role in catalyzing C−O and C−C cleavages as well as hydrogenation reactions, while the acidic sites of HZSM-5 facilitate dehydration and isomerization reactions. Additionally, the optimal MAB is crucial for tuning the activity and product selectivity. With this bifunctional catalyst system, a wide scope of substrates, including bottles, textile fibers, pellets, sheets, CDs/DVDs, postconsumer plastics with or without cleaning, plastics with pigments and even their various mixed plastic wastes can be efficiently converted into naphthenes with a high yield up to 99% at 250 °C and 4 MPa H_2 within 4−6 h. Furthermore, this catalyst exhibits excellent recyclability and maintains constant catalytic activity even after five repeated reactions. The one-pot HDO process with cost-effective and recoverable catalyst design offers an innovative approach toward highly efficient chemical recycling/upcycling of mixed plastics into valuable products, thereby significantly enhancing commercial viability of plastic wastes upcycling.

MATERIALS AND METHODS

Chemicals and Materials

$Ni(NO_3)_2{\cdot}6H_2O$ (98 wt %) and cyclopentane (C_5H_{10}, ≥ 96.0%) were supplied by Aladdin Chemical Reagent Co. Ltd. Ethylene glycol (AR, EG) was purchased from Tianjin Kemiou Chemical Reagent Co., Ltd. Polyphenylene oxide (PPO) and *n*-tetradecane ($C_{14}H_{30}$, ≥ 98.0%) were obtained from Shanghai Macklin Biochemical Technology Co., Ltd. *p*-Xylene was provided by Meryer (Shanghai) Chemical Technology Co., Ltd. Polyethylene terephthalate (PET), DMT (99%), ethyl 4-methylbenzoate (99%), methyl 4-methylbenzoate (98%), and 4-methylbenzoic acid (98%) were acquired from Heowns (Tianjin). 4-Methylcyclohexanemethanol was supplied by Tokyo Chemical Industry Co. Ltd. The HZSM-5 zeolites (SiO_2/Al_2O_3 = 25, 130, 200, 360, 470, and 1500) were purchased from Nankai University Catalyst Co. Ltd. All the real plastic wastes, including DVD, CD, PC sheet, Coca-Cola PET bottle, green Sprite PET bottle, PET white fiber, and PET red fiber, are provided by various Chinese vendors. Before conducting activity tests using real plastic wastes, they were cut into small pieces followed by washing them three times with water and ethanol, respectively. The metal layer on CD's and DVD disks was removed using sandpaper prior to cutting. Furthermore, it should be noted that the Coca-Cola PET bottle containing food residue was directly used after being cut into small pieces.

Catalysts Preparation

The Ni/HZSM-5 catalyst was prepared by using the ethylene glycol (EG)-assisted impregnation method. HZSM-5 with different SiO_2/Al_2O_3 (molar ratio = 25, 130, 200, 360, 470, 1500) were chosen as supports. The nickel loading was kept at 15 wt %. Initially, HZSM-5 was pretreated by calcination in a muffle furnace at 550 °C for 4 h at a ramping rate of 2 °C/min. Subsequently, HZSM-5 was impregnated with a specific amount of mixed $Ni(NO_3)_2$ and EG aqueous solution. The molar ratio between $Ni(NO_3)_2$ and EG was maintained at 1:1. After evaporation on a hot plate at 65 °C and drying in an oven at 80 °C for 12 h, the Ni/HZSM-5 catalyst was obtained through calcination in a muffle oven under an air atmosphere at 500 °C for 3 h with a heating rate of 2 °C/min. Reduction of the Ni/HZSM-5 catalyst was performed under a flow of H_2 (30 mL/min) at 500 °C for 2 h with a heating rate of 10 °C/min, followed by cooling down to room temperature using N_2 flow. After passivation with 2% O_2/N_2, the catalyst was ready for the HDO activity tests. The catalysts were

https://doi.org/10.1021/jacsau.4c00701
JACS Au 2024, 4, 4361−4373

labeled Ni/HZSM-5(x), where x represents the SiO_2/Al_2O_3 ratio. The Ni/Silicalite-1 catalyst without Brønsted acidic sites was also prepared by using a pure silicious zeolite support (Silicalite-1).

Activity Tests

The HDO of plastic waste was conducted in a 50 mL batch reactor (Anhui Kemi Instrument Co., Ltd.) with a glass liner and a magnetic stirrer. In each experiment, 0.3 g of plastic waste, 15 mL of cyclopentane, and 0.3 g of catalyst were loaded into the glass liner. Subsequently, the reactor was pressurized with N_2 (1 MPa) three times to remove air. After that, the reactor was filled to 4 MPa with H_2. The HDO test was performed at 240 °C and 500 rpm. After a specific reaction time, the reactor was rapidly cooled to room temperature using an ice−water bath for a quenching purpose. Then, the pressure was released and the liquid product along with a spent catalyst were collected by adding 10 mL cyclopentane containing *n*-tetradecane as an internal standard compound. The structures of products were identified by using GC−MS analysis using a Shimadzu GCMS-QP2020 instrument, equipped with a Rtx-5MS capillary column. Quantitative analysis of the liquid products was performed using an Agilent 7890A GC instrument equipped with an HP-PONA column and a flame ionization detector (FID). The gaseous products were analyzed by a Shimadzu 2014 GC system with a TCD detector and an FID detector using a packed column (carbon molecular sieve TDX-01) and a PLOT Q capillary column, respectively.

The HDO reactions of model compounds were conducted by following a similar procedure. To prevent any initial hydrogenation reactions during the heating process, the reactor was initially pressurized with 0.5 MPa of N_2 until reaching the desired temperature and then further pressurized with an additional 4 MPa of H_2. Control experiments confirmed the negligible reaction occurrence during the heating phase under a N_2 atmosphere.

The conversion, the yield of all products, and carbon balance (C. B.) from HDO reactions were calculated on a carbon basis using the following equations

$$\text{conversion [\%]} = \frac{\text{mol of initial reactant} - \text{mol of unreacted reactant}}{\text{mole of initial reactant}} \times 100$$

$$\text{yield of detected products [\%-C]} = \frac{\text{mol}_{\text{product}} \times \text{C atoms in product}}{\text{mol of total C atoms of initial aromatic reactants}} \times 100$$

$$\text{carbon balance [\%-C]} = \frac{\text{mol of total C atoms in all detected products}}{\text{mol of total C atoms of initial aromatic reactants}} \times 100$$

The control experiment using only solvents with the Ni/HZSM-5(360) catalyst showed that the ring-opening products (2-methylbutane and *n*-pentane) and C−C cracking products (*n*-butane, propane, ethane, and methane) were formed (Figure S12). However, these observed products were limited to C_1−C_5 alkanes, which have no impact on carbon balances or yields in this study. In addition, given the cracking of the solvent, the gas products are not calculated. The yield and carbon balance are calculated based on the reachable maximum carbon number of aromatic monomer segments. The response factor for each product was determined through calibration using standard compounds at varying concentrations.

The catalysts used were collected by centrifugation in the recyclability tests. Subsequently, the obtained spent catalysts were washed with 10 mL of cyclopentane three times, followed by drying at 80 °C for 12 h and calcination at 500 °C for 3 h with a ramping rate of 10 °C/min. Prior to the activity test, the catalyst was subjected to reduction and passivation once again.

Catalysts Characterizations

The structural properties of the catalysts were determined by using XRD (D8 Focus, Bruker) with Cu Kα radiation (λ = 1.541 Å) at 40 kV and 40 mA in the 2θ range from 10 to 80° with a scanning speed of 8°/min. The morphology and structure of the catalysts were characterized by SEM (Apreo S, FEI) and TEM (JEM-2100F, JEOL).

The metal dispersions of Ni/HZSM-5 catalysts were determined by hydrogen chemisorption using a dynamic pulse method. Prior to testing, catalyst samples (0.1 g) were in situ reduced at 500 °C for 2 h (10 °C/min) in 30 mL/min H_2 flow and subsequently cooled to 50 °C in Ar flow (30 mL/min). Then, pure H_2 doses were introduced until a complete saturation was achieved. Finally, Ar was passed through the reactor to remove the weakly adsorbed H_2 from the catalyst. The surface nickel atom on the Ni/HZSM-5 catalyst was determined based on a stoichiometry of one hydrogen atom per surface nickel atom by H_2 chemisorption.[52] The metal dispersion was calculated based on the following equation

$$D = n_{\text{surface}}/n_{\text{total}} \times 100\%$$

n_{surface}: the number of surface nickel atom in the catalyst and n_{total}: the total number of nickel atom in the catalyst.

The acid type and concentration were determined by using a Bruker Tensor 27 IR spectrometer through pyridine adsorption. The catalyst was pressed into a disc with a diameter of approximately 12.2 mm using a mold, which was then placed in an infrared cell connected to a closed glass vacuum system. The sample underwent pretreatment at 400 °C for 60 min under vacuum conditions to remove any adsorbed species. Subsequently, it was cooled to room temperature under vacuum (10^{-2} Pa), and the reference spectrum was recorded. Following this, pyridine vapor was introduced to the catalyst, until saturation adsorption occurred. Desorption took place by heat-treating the adsorbed sample at a heating rate of 5 °C/min, and IR spectra were recorded at temperatures of 100, 150, 200, 300, and 350 °C, respectively, during this process. Spectra were recorded with a resolution of 4 cm^{-1} and coaddition of 64 scans. The concentrations of Brønsted acid and Lewis acid sites were determined following the method described by Emeis,[53] which involved calculating the integrated absorbance values at wavenumber of 1540 and 1450 cm^{-1}, respectively.

The coke deposition on the spent catalysts was quantified by employing thermogravimetric analysis (TGA, TA Q500) under a flowing air stream of 50 mL/min at a heating rate of 10 °C/min. Prior to analysis, the spent Ni/HZSM-5(360) catalyst underwent three cycles of washing with cyclopentane and ethanol to eliminate weakly adsorbed reactants, followed by drying at 80 °C for 12 h.

■ ASSOCIATED CONTENT

Supporting Information

The Supporting Information is available free of charge at https://pubs.acs.org/doi/10.1021/jacsau.4c00701.

HDO of PET over various catalysts; characterizations of Ni/HZSM-5(360) and Ni/HZSM-5(360)-NE catalysts; GC chart for the gas products from HDO of PET and hydroconversion of the solvent over Ni/HZSM-5(360); reaction profile of EMB over the Ni/HZSM-5(360) catalyst; reaction pathway for HDO of EMB over the Ni/HZSM-5(360) catalyst; reaction pathway for HDO of DMT over the Ni/HZSM-5(360) catalyst; HDO of PET over Ni/HZSM-5(360) and Ni/HZSM-5(360)-NE catalysts at short reaction time (1 h); SEM images of HZSM-5 and the reduced Ni/HZSM-5 catalysts; reaction rates of C_8−OH conversion catalyzed over different catalysts; characterizations of used Ni/HZSM-5(360) catalyst; chemical structure examples of red dyes; HDO of PPO over the Ni/HZSM-5(360) catalyst; reaction profile of PPO over the Ni/HZSM-5(360) catalyst and the reaction pathway for HDO of PPO; and GC chart for the solvent and liquid and gas products from hydroconversion of the solvent over Ni/HZSM-5(360) (PDF)

https://doi.org/10.1021/jacsau.4c00701
JACS Au 2024, 4, 4361−4373

AUTHOR INFORMATION

Corresponding Authors

Sibao Liu − *Engineering Research Center of Polymer Green Recycling of Ministry of Education, Fujian Key Laboratory of Pollution Control & Resource Reuse, College of Environmental and Resources, Fujian Normal University, Fuzhou 350007 Fujian, China;* orcid.org/0000-0001-9735-3491; Email: liusibao@fjnu.edu.cn

Guozhu Liu − *Key Laboratory for Green Chemical Technology of Ministry of Education, School of Chemical Engineering and Technology, Tianjin University, Tianjin 300072, China; Haihe Lab of Sustainable Chemical Transformations, Tianjin 300192, China;* orcid.org/0000-0003-2193-5289; Email: gliu@tju.edu.cn

Authors

Jieyi Liu − *Key Laboratory for Green Chemical Technology of Ministry of Education, School of Chemical Engineering and Technology, Tianjin University, Tianjin 300072, China*

Nan Wang − *Key Laboratory for Green Chemical Technology of Ministry of Education, School of Chemical Engineering and Technology, Tianjin University, Tianjin 300072, China*

Complete contact information is available at: https://pubs.acs.org/10.1021/jacsau.4c00701

Author Contributions

[‖]J.L. and N.W. contributed equally to this work. Sibao Liu and Guozhu Liu conceived the project and designed the experiments. Jieyi Liu and Nan Wang executed all the experiments. Nan Wang reproduced some experiments. Sibao Liu, Jieyi Liu, and Nan Wang wrote the article. Sibao Liu and Guozhu Liu reviewed and edited the article. All the authors proofread the manuscript.

Notes

The authors declare no competing financial interest.

ACKNOWLEDGMENTS

We thank the National Natural Science Foundation of China (22208243, 52276209) for financial support.

REFERENCES

(1) Agrawala, S., Co-operation, O. F. E. *Global Plastics Outlook Policy Scenarios to 2060*; OECD Publishing, 2022.

(2) Kwon, D. Three ways to solve the plastics pollution crisis. *Nature* **2023**, *616*, 234−237.

(3) MacLeod, M.; Arp, H. P. H.; Tekman, M. B.; Jahnke, A. The global threat from plastic pollution. *Science* **2021**, *373* (6550), 61−65.

(4) Santos, R. G.; Machovsky-Capuska, G. E.; Andrades, R. Plastic ingestion as an evolutionary trap: Toward a holistic understanding. *Science* **2021**, *373* (6550), 56−60.

(5) Korley, L. T.; Epps, T. H., III; Helms, B. A.; Ryan, A. J. Toward polymer upcycling-adding value and tackling circularity. *Science* **2021**, *373* (6550), 66−69.

(6) Geyer, R.; Jambeck, J. R.; Law, K. L. Production, use, and fate of all plastics ever made. *Sci. Adv.* **2017**, *3* (7), No. e1700782.

(7) Jehanno, C.; Alty, J. W.; Roosen, M.; De Meester, S.; Dove, A. P.; Chen, E. Y. X.; Leibfarth, F. A.; Sardon, H. Critical advances and future opportunities in upcycling commodity polymers. *Nature* **2022**, *603* (7903), 803−814.

(8) Dong, Z.; Chen, W.; Xu, K.; Liu, Y.; Wu, J.; Zhang, F. Understanding the Structure−Activity Relationships in Catalytic Conversion of Polyolefin Plastics by Zeolite-Based Catalysts: A Critical Review. *ACS Catal.* **2022**, *12* (24), 14882−14901.

(9) Arifuzzaman, M.; Sumpter, B. G.; Demchuk, Z.; Do, C.; Arnould, M. A.; Rahman, M. A.; Cao, P.-F.; Popovs, I.; Davis, R. J.; Dai, S.; Saito, T. Selective deconstruction of mixed plastics by a tailored organocatalyst. *Mater. Horiz.* **2023**, *10* (9), 3360−3368.

(10) Zhao, B.; Tan, H.; Yang, J.; Zhang, X.; Yu, Z.; Sun, H.; Wei, J.; Zhao, X.; Zhang, Y.; Chen, L.; Yang, D.; Deng, J.; Fu, Y.; Huang, Z.; Jiao, N. Catalytic conversion of mixed polyolefins under mild atmospheric pressure. *Innovation* **2024**, *5* (2), 100586.

(11) Lee, K.; Jing, Y.; Wang, Y.; Yan, N. A unified view on catalytic conversion of biomass and waste plastics. *Nat. Rev. Chem* **2022**, *6* (9), 635−652.

(12) Ellis, L. D.; Rorrer, N. A.; Sullivan, K. P.; Otto, M.; McGeehan, J. E.; Román-Leshkov, Y.; Wierckx, N.; Beckham, G. T. Chemical and biological catalysis for plastics recycling and upcycling. *Nat. Catal.* **2021**, *4* (7), 539−556.

(13) Zhang, W.; Kim, S.; Wahl, L.; Khare, R.; Hale, L.; Hu, J.; Camaioni, D. M.; Gutiérrez, O. Y.; Liu, Y.; Lercher, J. A. Low-temperature upcycling of polyolefins into liquid alkanes via tandem cracking-alkylation. *Science* **2023**, *379* (6634), 807−811.

(14) Wei, J.; Liu, J.; Zeng, W.; Dong, Z.; Song, J.; Liu, S.; Liu, G. Catalytic hydroconversion processes for upcycling plastic waste to fuels and chemicals. *Catal. Sci. Technol.* **2023**, *13* (5), 1258−1280.

(15) Gan, L.; Dong, Z.; Xu, H.; Lv, H.; Liu, G.; Zhang, F.; Huang, Z. Beyond conventional degradation: catalytic solutions for polyolefin upcycling. *CCS Chem.* **2024**, *6* (2), 313−333.

(16) Liu, S.; Kots, P. A.; Vance, B. C.; Danielson, A.; Vlachos, D. G. Plastic waste to fuels by hydrocracking at mild conditions. *Sci. Adv.* **2021**, *7* (17), No. eabf8283.

(17) Xu, Z.; Munyaneza, N. E.; Zhang, Q.; Sun, M.; Posada, C.; Venturo, P.; Rorrer, N. A.; Miscall, J.; Sumpter, B. G.; Liu, G. Chemical upcycling of polyethylene, polypropylene, and mixtures to high-value surfactants. *Science* **2023**, *381* (6658), 666−671.

(18) Barnard, E.; Arias, J. J. R.; Thielemans, W. Chemolytic depolymerisation of PET: a review. *Green Chem.* **2021**, *23* (11), 3765−3789.

(19) Kratish, Y.; Marks, T. J. Efficient polyester hydrogenolytic deconstruction via tandem catalysis. *Angew. Chem., Int. Ed.* **2022**, *61* (9), No. e202112576.

(20) Kratish, Y.; Li, J.; Liu, S.; Gao, Y.; Marks, T. J. Polyethylene terephthalate deconstruction catalyzed by a carbon-supported single-site molybdenum-dioxo complex. *Angew. Chem., Int. Ed.* **2020**, *59* (45), 19857−19861.

(21) Sun, Z.; Wang, K.; Lin, Q.; Guo, W.; Chen, M.; Chen, C.; Zhang, C.; Fei, J.; Zhu, Y.; Li, J.; et al. Value-added upcycling of PET to 1, 4-cyclohexanedimethanol by a hydrogenation/hydrogenolysis relay catalysis. *Angew. Chem., Int. Ed.* **2024**, *63*, No. e202408561.

(22) Cheng, J.; Xie, J.; Xi, Y.; Wu, X.; Zhang, R.; Mao, Z.; Yang, H.; Li, Z.; Li, C. Selective upcycling of polyethylene terephthalate towards high-valued oxygenated chemical methyl *p*-methyl benzoate using a Cu/ZrO_2 catalyst. *Angew. Chem., Int. Ed.* **2024**, *63*, No. e202319896.

(23) Jing, Y.; Wang, Y.; Furukawa, S.; Xia, J.; Sun, C.; Hülsey, M. J.; Wang, H.; Guo, Y.; Liu, X.; Yan, N. Towards the circular economy: converting aromatic plastic waste back to arenes over a Ru/Nb_2O_5 catalyst. *Angew. Chem., Int. Ed.* **2021**, *60* (10), 5527−5535.

(24) Wei, J.; Zhu, M.; Liu, B.; Wang, N.; Liu, J.; Tomishige, K.; Liu, S.; Liu, G. Hydrodeoxygenation of oxygen-containing aromatic plastic wastes to liquid organic hydrogen carriers. *Angew. Chem., Int. Ed.* **2023**, *62* (46), No. e202310505.

(25) Wang, N.; Liu, J.; Liu, S.; Liu, G. Hydrodeoxygenation of oxygen-containing aromatic plastic wastes into cycloalkanes and aromatics. *ChemPlusChem* **2024**, *89*, No. e202400190.

(26) Ye, M.; Li, Y.; Yang, Z.; Yao, C.; Sun, W.; Zhang, X.; Chen, W.; Qian, G.; Duan, X.; Cao, Y.; et al. Ruthenium/TiO_2-catalyzed hydrogenolysis of polyethylene terephthalate: reaction pathways dominated by coordination environment. *Angew. Chem., Int. Ed.* **2023**, *62* (19), No. e202301024.

(27) Li, R.; Zeng, W.; Zhao, R.; Zhao, Y.; Wang, Y.; Zhang, F.; Tang, M.; Wang, Y.; Chang, X.; Wu, F.; et al. TiO2 nanoparticle supported

Ru catalyst for chemical upcycling of polyethylene terephthalate to alkanes. *Nano Res.* **2023**, *16*, 12223−12229.
(28) Gao, Z.; Ma, B.; Chen, S.; Tian, J.; Zhao, C. Converting waste PET plastics into automobile fuels and antifreeze components. *Nat. Commun.* **2022**, *13* (1), 3343.
(29) Li, Y.; Wang, M.; Liu, X.; Hu, C.; Xiao, D.; Ma, D. Catalytic transformation of PET and CO_2 into high-value chemicals. *Angew. Chem., Int. Ed.* **2022**, *61* (10), No. e202117205.
(30) Liang, X.; Wang, M.; Ma, D. One-pot conversion of polyester and carbonate into formate without external H2. *J. Am. Chem. Soc.* **2024**, *146* (4), 2711−2717.
(31) Vardon, D. R.; Sherbacow, B. J.; Guan, K.; Heyne, J. S.; Abdullah, Z. Realizing "net-zero-carbon" sustainable aviation fuel. *Joule* **2022**, *6* (1), 16−21.
(32) Muldoon, J. A.; Harvey, B. G. Bio-based cycloalkanes: the missing link to high-performance sustainable jet fuels. *ChemSusChem* **2020**, *13* (22), 5777−5807.
(33) Zhou, M. J.; Miao, Y.; Gu, Y.; Xie, Y. Recent advances in reversible liquid organic hydrogen carrier systems: from hydrogen carriers to catalysts. *Adv. Mater.* **2024**, *36*, 2311355.
(34) Tang, H.; Li, N.; Li, G.; Wang, A.; Cong, Y.; Xu, G.; Wang, X.; Zhang, T. Synthesis of gasoline and jet fuel range cycloalkanes and aromatics from poly (ethylene terephthalate) waste. *Green Chem.* **2019**, *21* (10), 2709−2719.
(35) Tang, H.; Hu, Y.; Li, G.; Wang, A.; Xu, G.; Yu, C.; Wang, X.; Zhang, T.; Li, N. Synthesis of jet fuel range high-density polycycloalkanes with polycarbonate waste. *Green Chem.* **2019**, *21* (14), 3789−3795.
(36) Wang, J.; Jiang, J.; Dong, X.; Zhang, Y.; Yuan, X.; Meng, X.; Zhan, G.; Wang, L.; Wang, Y.; Ragauskas, A. J. Catalytic cascade vapor-phase hydrotreatment of plastic waste into fuels and its sustainability assessment. *Green Chem.* **2022**, *24* (21), 8562−8571.
(37) Wang, L.; Han, F.; Li, G.; Zheng, M.; Wang, A.; Wang, X.; Zhang, T.; Cong, Y.; Li, N. Direct synthesis of a high-density aviation fuel using a polycarbonate. *Green Chem.* **2021**, *23* (2), 912−919.
(38) Murali, V.; Kim, J. R.; Park, Y.-K.; Ha, J.-M.; Jae, J. Water-assisted single-step catalytic hydrodeoxygenation of polyethylene terephthalate into gasoline-and jet fuel-range cycloalkanes over supported Ru catalysts in a biphasic system. *Green Chem.* **2023**, *25* (21), 8570−8583.
(39) Luo, J.-H.; Deng, J. Direct synthesis of a jet fuel range dicycloalkane from polycarbonate waste at a high concentration. *ACS Sustain. Chem. Eng.* **2023**, *11* (48), 17120−17129.
(40) Manal, A. K.; Shanbhag, G. V.; Srivastava, R. Design of a bifunctional catalyst by alloying Ni with Ru-supported H-beta for selective hydrodeoxygenation of bisphenol A and polycarbonate plastic waste. *Appl. Catal., B* **2023**, *338*, 123021.
(41) Wang, L.; Li, G.; Cong, Y.; Wang, A.; Wang, X.; Zhang, T.; Li, N. Direct synthesis of a jet fuel range dicycloalkane by the aqueous phase hydrodeoxygenation of polycarbonate. *Green Chem.* **2021**, *23* (10), 3693−3699.
(42) Wang, M.; Gao, Y.; Yuan, S.; Deng, J.; Yang, J.; Yan, J.; Yu, S.; Xu, B.; Ma, D. Complete hydrogenolysis of mixed plastic wastes. *Nat. Chem. Eng.* **2024**, *1*, 376−384.
(43) Zhang, Z.; Wang, J.; Ge, X.; Wang, S.; Li, A.; Li, R.; Shen, J.; Liang, X.; Gan, T.; Han, X.; et al. Mixed plastics wastes upcycling with high-stability single-atom Ru catalyst. *J. Am. Chem. Soc.* **2023**, *145* (41), 22836−22844.
(44) Qiu, Z.; Lin, S.; Chen, Z.; Chen, A.; Zhou, Y.; Cao, X.; Wang, Y.; Lin, B.-L. A reusable, impurity-tolerant and noble metal−free catalyst for hydrocracking of waste polyolefins. *Sci. Adv.* **2023**, *9* (25), No. eadg5332.
(45) Andini, E.; Bhalode, P.; Gantert, E.; Sadula, S.; Vlachos, D. G. Chemical recycling of mixed textile waste. *Sci. Adv.* **2024**, *10* (27), No. eado6827.
(46) El Darai, T.; Ter-Halle, A.; Blanzat, M.; Despras, G.; Sartor, V.; Bordeau, G.; Lattes, A.; Franceschi, S.; Cassel, S.; Chouini-Lalanne, N.; et al. Chemical recycling of polyester textile wastes: shifting towards sustainability. *Green Chem.* **2024**, *26*, 6857−6885.
(47) Munnik, P.; de Jongh, P. E.; de Jong, K. P. Recent Developments in the Synthesis of Supported Catalysts. *Chem. Rev.* **2015**, *115* (14), 6687−6718.
(48) Qiu, S.; Zhang, X.; Liu, Q.; Wang, T.; Zhang, Q.; Ma, L. A simple method to prepare highly active and dispersed Ni/MCM-41 catalysts by co-impregnation. *Catal. Commun.* **2013**, *42*, 73−78.
(49) Borg, Ø.; Dietzel, P. D. C.; Spjelkavik, A. I.; Tveten, E. Z.; Walmsley, J. C.; Diplas, S.; Eri, S.; Holmen, A.; Rytter, E. Fischer−Tropsch synthesis: Cobalt particle size and support effects on intrinsic activity and product distribution. *J. Catal.* **2008**, *259* (2), 161−164.
(50) Koizumi, N.; Suzuki, S.; Niiyama, S.; Ibi, Y.; Shindo, T.; Yamada, M. Effects of glycols on Fischer−Tropsch synthesis activity and coordination structure of Co species in Co/SiO2: Mechanism for enhanced dispersion of Co0 nanoparticles. *Appl. Catal., A* **2011**, *395* (1−2), 138−145.
(51) Liu, J.; Wei, J.; Feng, X.; Song, M.; Shi, S.; Liu, S.; Liu, G. Ni/HZSM-5 catalysts for hydrodeoxygenation of polycarbonate plastic wastes into cycloalkanes for sustainable aviation fuels. *Appl. Catal., B* **2023**, *338*, 123050.
(52) Bartholomew, C. H.; Pannell, R. B. The stoichiometry of hydrogen and carbon monoxide chemisorption on alumina- and silica-supported nickel. *J. Catal.* **1980**, *65* (2), 390−401.
(53) Emeis, C. A. Determination of Integrated Molar Extinction Coefficients for Infrared Absorption Bands of Pyridine Adsorbed on Solid Acid Catalysts. *J. Catal.* **1993**, *141* (2), 347−354.

https://doi.org/10.1021/jacsau.4c00701
JACS Au 2024, 4, 4361−4373